

Spectrum of Surgically Resected Lesions of the Cavernous Sinus: A Neuropathologic Audit

Chandrashekhar T. Nagaraja¹ Arvinda H. Ramalingaiah^{2,*} Arivazhagan Arimappamagan³
Saikat Mitra⁴ Dhaval Shukla³ Dwarakanath Srinivas³ Shankar S. Krishna⁴ Anita Mahadevan^{4,*}

¹ Department of Pathology, Shimoga Institute of Medical Sciences, Shivammoga, Karnataka, India

² Departments of Neuroimaging and Interventional Radiology, National Institute of Mental Health and Neurosciences, Bengaluru, Karnataka, India

³ Departments of Neurosurgery, National Institute of Mental Health and Neurosciences, Bengaluru, Karnataka, India

⁴ Departments of Neuropathology, National Institute of Mental Health and Neurosciences, Bengaluru Karnataka, India

Address for correspondence Anita Mahadevan, MD, Department of Neuropathology, National Institute of Mental Health and Neurosciences, Bengaluru 560029, Karnataka, India (e-mail: mahadevananita@gmail.com).

J Neurosci Rural Pract 2022;13:495–509.

Abstract

Background The cavernous sinus is a complex space composed of extradural venous plexus within dural folds. Several important structures like the carotid artery, cranial nerves, and sympathetic nerve fibers traverse through this space. Radiological diagnosis may not be definitive and in the context of discordance between clinical and neuroimaging diagnosis, histopathological evaluation becomes essential for diagnosis and management. Literature on the pathological spectrum of lesions is scarce as, with a shift in the treatment paradigm, most small lesions of cavernous sinus are treated with radiosurgery. However, surgical management still plays a role for larger lesions and in radiologically ambiguous cases for planning the definitive management.

Materials and Methods We retrospectively reviewed all surgically resected lesions of the cavernous sinus over the last two decades (1998–2019). The clinical presentation, neuroimaging features, and histopathological findings were reviewed. Lesions extending from sella and other adjacent areas were excluded.

Results Thirty-eight cases of isolated cavernous sinus mass lesions were diagnosed over the last two decades (1998–2019). Cavernous hemangiomas (19 cases, 50%) constituted the most frequent pathology, followed by aspergilloma, meningioma, schwannoma, metastatic adenocarcinoma, chondrosarcoma, and chordoma. Overall, 29.4% (10/34) could not be accurately diagnosed on neuroimaging. Of these, four cases of cavernous hemangiomas were mistaken for either meningioma (three cases) or schwannoma (one case). Neither chordoma nor chondrosarcoma was suspected.

Keywords

- ▶ histopathology
- ▶ cavernous sinus
- ▶ imaging

* These authors have equally contributed to the work.

DOI <https://doi.org/10.1055/s-0042-1750707>.
ISSN 0976-3147.

© 2022. Association for Helping Neurosurgical Sick People. All rights reserved.

This is an open access article published by Thieme under the terms of the Creative Commons Attribution-NonDerivative-NonCommercial-License, permitting copying and reproduction so long as the original work is given appropriate credit. Contents may not be used for commercial purposes, or adapted, remixed, transformed or built upon. (<https://creativecommons.org/licenses/by-nc-nd/4.0/>)

Thieme Medical and Scientific Publishers Pvt. Ltd., A-12, 2nd Floor, Sector 2, Noida-201301 UP, India

Conclusion This is the first study in literature, enumerating the pathological and imaging spectrum of surgically resected cavernous sinus lesions. Cavernous hemangiomas, metastases and chordomas, and chondrosarcoma posed the greatest difficulty in diagnosis on neuroimaging and the reasons for the same are analyzed. In the context of clinical and neuroimaging discordance in diagnosis, pathological characterization becomes essential for appropriate and timely management.

Introduction

The cavernous sinus is a complex space composed of extradural venous plexus within dural folds. Several important structures like carotid artery, cranial nerves, and sympathetic nerve fibers traverse through this space. These diverse structures can potentially give rise to a broad spectrum of lesions and diseases that produces cavernous sinus syndrome.¹ The mass lesion spectrum includes infectious diseases (bacterial and fungal), inflammatory lesions (Tolosa–Hunt syndrome and inflammatory pseudotumors), vascular lesions (carotid aneurysms and carotid–cavernous fistulas), and neoplasms.^{1,2} Cavernous sinus tumors most commonly causes cavernous sinus syndrome. Several primary tumors (meningioma, schwannoma, and hemangioma) and secondary metastatic tumor deposits are described.^{1,3} Cavernous sinus syndrome is characterized by a plethora of clinical manifestations: ophthalmoplegia, chemosis, proptosis, Horner's syndrome, or trigeminal sensory loss. Determining the exact etiology is a challenge as radiological findings may not be definitive and in the context of discordance between clinical and neuroimaging diagnosis, histopathological evaluation is often essential for planning treatment. The management of cavernous sinus lesions poses a formidable challenge due to vascularity and complex neurovascular structures.⁴ Extensive literature is available as individual case reports and describes the management and radiological features, little has been published regarding the pathological spectrum of lesions in this area.^{1,3–9} With recent advances in radiosurgical techniques, the treatment of choice, particularly for smaller lesions (<10 cc) is radiosurgery with significantly lower morbidity. However, surgical pathology still has a critical role in evaluating radiologically ambiguous cases and for larger lesions undergoing surgical management for planning the definitive management.

In this report, we illustrate the spectrum of the pathologies involving cavernous sinus among the cases managed surgically and review the imaging features and histopathological features.

Materials and Methods

We retrospectively retrieved all surgically resected lesions of the cavernous sinus between 1998 and 2019 from the pathology records. The demographic details, clinical presentation, neuroimaging features, and histopathology were reviewed. Lesions extending from sella and other adjacent areas were excluded.

Results

Thirty-eight cases of isolated cavernous sinus mass lesions were operated on over the last 20 years (1998–2019), constituting 0.075% (38/50,406) of all surgical biopsies received in that period. The mean age at presentation was 34.9 years (range: 5–73 years) with female preponderance (male-to-female [M:F] ratio = 1:2.16). The majority of patients were between the third and sixth decade (18 cases, 47.36%). On histologic evaluation, cavernous hemangioma (19 cases, 50%) constituted the most frequent pathology, followed by aspergilloma (five cases, 13.15%), meningioma (five cases, 13.15%), schwannoma (three cases, 7.89%), metastatic deposits of adenocarcinoma (three cases, 7.89%), chondrosarcoma (two cases, 5.26%), and a single case of chordoma (2.63%). The histological spectrum, clinical profile, and imaging features of various cavernous sinus mass lesions are summarized in ▶Table 1.

Cavernous Hemangioma

Incidence peaked in during third and fourth decades (6 cases, 31.57%; 19 cases, 50%; age range: 5–65 years; mean = 36.42 years; M:F = 1:2.8]. Clinically, features of raised intracranial pressure were common and included headache (75%), blurring of vision (37.5%), followed by ptosis (60%), diplopia (33.3%), facial numbness (33.3%), and dystonia (6.6%) with a mean duration of symptoms being 1 year. Multiple cranial nerve palsies (total ophthalmoplegia = 33.3%, third and sixth nerve palsy = 20%, isolated fifth nerve palsy = 13.3%, and isolated third nerve palsy = 20%) were frequent. On cranial computed tomography (CT) and magnetic resonance imaging (MRI), most were well circumscribed. On MRI, all lesions were iso-hypointense on T1-weighted imaging (WI) and brilliantly hyperintense on T2WI and fluid-attenuated inversion recovery (FLAIR) showing exuberant enhancement on contrast administration (▶Fig. 1A–D). Few lesions showed early central nonenhancing areas which enhanced in the delayed images. These lesions insinuated the surrounding structures without causing destruction. On CT scans, bony remodeling was seen with the lesion appearing hyper- to isodense. On neuroimaging, four cases of cavernous hemangiomas were mistaken for meningioma (three cases) or schwannoma (one case). Histologically, the lesions appeared partially circumscribed by a collagenous capsule drawn from the cavernous sinus dural wall (▶Fig. 1E). Microscopically showed vascular channels of varying caliber arranged back to back in a lobular manner (▶Fig. 1E). The channels were lined by prominent endothelium. The lumina were widely

Table 1 Clinical, neuroimaging, and pathology of cavernous sinus lesions

No.	Age/sex	Clinical features	O/E	CT	MRI	R/D	HPE
1	57/F	Headache, diplopia, ptosis	Right: III nerve palsy, left V1 hypoesthesia	Circumscribed, isodense, homogenous contrast enhancement	Circumscribed, T1-hypo- and T2-hyperintense	Meningioma	Vascular meningioma
2	45/M	Headache, diplopia, ptosis	Fifth nerve palsy	Poorly circumscribed, hyperdense, homogenous contrast enhancement	ND	Cavernous hemangioma	Cavernous angioma
3	42/F	Headache, ocular pain, visual loss	third and sixth nerve palsy left side	ND	Poorly circumscribed, hypointense lesion with central hyperintensity on T1, homogenous contrast enhancement	Cavernous hemangioma	Cavernous angioma
4	73/M	Memory loss, headache, giddiness, visual loss	Short-term memory loss	ND	Circumscribed, hyperintense on T2		Metastatic adenocarcinoma
5	5/M	Diplopia, visual loss, sensory disturbances, headache	Left sixth nerve palsy	ND	Circumscribed, hyperintense lesion, homogenous contrast enhancement	Cavernous hemangioma	Cavernous angioma
6	25/F	Pain, sensory disturbances	ND	Ill circumscribed, enhancing irregularly	ND	Aspergilloma	Aspergilloma
7	53/F	Pain, ptosis, visual loss	Total ophthalmoplegia. second–fourth and sixth nerve palsy left	Ill circumscribed, enhancing irregularly	ND	Meningioma	Fungal sinusitis, aspergillosis
8	17/F	Headache, amenorrhoea, visual loss	Right eye, total loss of vision; left eye, temporal hemianopia	Isodense, homogenous enhancement, calcified	Iso on T1, hyperintense, homogenous contrast enhancement	Cavernous hemangioma	Cavernous hemangioma
9	32/F	Ptosis, visual loss	Left third nerve palsy with pupillary sparing	ND	Hypointense on T1 and hyperintense on T2, homogenous contrast enhancement	Meningioma	Cavernous hemangioma
10	49/F	Headache, giddiness	Left third and sixth nerve palsy	ND	Hypo on T1, hyper on T2 lesion, homogenous contrast enhancement	Schwannoma	Cavernous hemangioma
11	20/F	Headache, ptosis, visual loss	Conscious, oriented, left ptosis with total ophthalmoplegia, palsy	Well circumscribed, homogenous enhancement	Isointense on T1 and hyperintense on T2, homogenous contrast enhancement	Cavernous hemangioma	Cavernous hemangioma
12	28/F	Headache, ptosis, facial dystonia	Left third, fourth, and sixth nerve palsy, fifth motor sensory paresis	Isodense, Homogenous enhancement	Hypointense on T1, hyperintense on T2 erosion of petrous, homogenous contrast enhancement	Cavernous hemangioma	Cavernous hemangioma

(Continued)

Table 1 (Continued)

No.	Age/sex	Clinical features	O/E	CT	MRI	R/D	HPE
13	24/M	Sensorimotor trigeminal neuropathy, slowly progressive	NA	NA	NA	NA	Aspergilloma
14	49/F	Headache	NA	NA	NA	NA	Aspergilloma
15	19/F	Headache	Left third, fourth, and sixth nerve palsy	NA	NA	NA	Vascular schwannoma
16	21/M	Double vision	Left sixth nerve palsy	NA	NA	NA	Cavernous angioma
17	22/M	NA	NA	NA	Right parasellar lesion, extending into sella, pituitary made out separately, grossly hyperintense on T2WI and FLAIR, isointense on T1WI, homogenous postcontrast enhancement with central few areas of nonenhancement. ICA is not narrowed.	Cavernous hemangioma. Right side DD: microcytic meningioma	Cavernous angioma
18	22/F	Left ptosis, left diplopia, headache, drowsiness	NA	ND	Left parasellar lesion with suprasellar extension. Large grossly hyperintense lesion on T2WI and FLAIR images, with central hypointense areas. Isointense on T1WI, heterogeneous exuberant postcontrast enhancement. No obvious blooming areas on SWI. Left cavernous and supraclinoid ICA is stretched with no obvious narrowing	Left cavernous hemangioma	Cavernous angioma
19	48/M	Diplopia, drooping of eyelid and vision loss in left eye	Left third-fifth nerve palsy. Left V1/V2 sensory deficit	ND	Left parasellar lesion, heterogeneously hyperintense on T2WI and FLAIR (not so hyperintense) with appearance of septations within it, hypointense on T1WI with heterogeneous enhancement with more non enhancing areas. Extension into foramen rotundum noted along left maxillary nerve. No areas of blooming noted. ICA not involved	Left trigeminal schwannoma DD: meningioma	Low-grade chondrosarcoma
20	20/M	Diplopia and vision loss in right eye	NA	ND	Right parasellar lesion, heterogeneously hyperintense on T2WI and FLAIR (few hypointense areas are also seen), hypointense on T1WI and showing heterogeneous post-contrast enhancement. (Not so hyperintense as was seen in hemangioma). Right cavernous ICA is stretched and narrowed.	Right-sided meningioma	Schwannoma

Table 1 (Continued)

No.	Age/sex	Clinical features	O/E	CT	MRI	R/D	HPE
21	58/F	Headache, photophobia, left eyelid drooping	left third, fourth, and sixth palsy, left V1 hyperesthesia	ND	Left sided parasellar lesion with sellar extension. Hyperintense on T2WI and FLAIR, hypointense on T1WI with exuberant postcontrast enhancement. No blooming areas noted. ICA is stretched without narrowing Incidentally, anterior falxine meningioma noted	Left cavernous hemangioma DD: meningioma in view of presence of one more meningioma	Hemangioma
22	40/F	Right facial paresthesia, numbness eye movement restriction and visual disturbance	-	ND	Right parasellar lesion with sellar extension. Uniformly hyperintense on T2WI and FLAIR Images with exuberant postcontrast enhancement. No blooming in SWI. Stretching of right ICA noted	Right cavernous hemangioma	Hemangioma
23	55/M	Pain, tingling, loss of sensation in left face	left proptosis, left second-fifth and seventh nerve involvement	ND	Limited films. Left parasellar lesion with orbital extension appearing hypointense on T2WI and FLAIR images and isointense on T1WI showing uniform enhancement with orbital extension also	Meningioma	Poorly differentiated adenocarcinoma
24	25/F	NA	NA	NA	Left parasellar lesion. Hypointense on T2WI and FLAIR images, isointense on T1WI with uniform postcontrast enhancement. Dural tail also noted	meningioma	Mets carcinoma
25	48/F	Facial paresthesia	Right-sided third nerve paralysis	ND	Right large parasellar lesion with suprasellar extension. Grossly hyperintense on T2WI and FLAIR, hypointense on T1WI no blooming on SWI images. ICA is stretched, heterogenous postcontrast enhancement with few non enhancing hypointense areas within it	Cavernous hemangioma	Cavernous hemangioma
26	28/M	Headache, left periorbital pain, left eye diplopia × year	-	ND	Left parasellar lesion, heterogenous signal intensity on T2WI and FLAIR images, grossly hyperintense cystic areas with solid isointense areas on T2WI and FLAIR and heterogenous postcontrast enhancement. ICA is stretched and narrowed. Blooming areas are seen on SWI images	Left fifth nerve schwannoma. DD meningioma	Schwannoma
27	24/F	Card NA	Cavernous sinus hemangioma (nonfunctioning)	ND	Left large parasellar lesion with suprasellar extension. Having both hypointense and hyperintense areas on T1WI and FLAIR images. Uniformly hypointense on T1WI. Showing exuberant post-contrast enhancement (both areas)	Cavernous hemangioma	Cavernous hemangioma

(Continued)

Table 1 (Continued)

No.	Age/sex	Clinical features	O/E	CT	MRI	R/D	HPE
28	46/F	Headache, left facial pain × 5 month, left eyelid drooping × 1 year,	Left MCA infarct	ND	Left parasellar lesion with suprasellar and posterior fossa extension. Appearing heterogeneously hyperdense on CT scan, hypointense on T2WI and FLAIR images, hypointense on T1WI, heterogeneous postcontrast enhancement. Narrowing of the ICA noted with stretching. No bony destruction seen. No blooming on SWI images	Meningioma DD: fungal lesion	Aspergillus
29	56/M	Right eyelid drooping × 10 month, diplopia × 2 months		Only CT images are available and appear hypodense with presence of calcifications	Right parasellar lesion with sellar and Meckel's cave extension. Appearing hyperintense on T2WI and FLAIR images with septations like appearance within it. Showing blooming on SWI images. Gross postcontrast enhancement is seen. It is hypointense on T1WI	Right trigeminal schwannoma	Low-grade chondrosarcoma
30	65 Y/M	drooping of left eyelid, left eye loss of vision for 2 weeks, one episode of seizure, left V1 paresthesia	-	ND	Left parasellar lesion with suprasellar extension. Large lesion with homogenous hyperintensity on T2WI and FLAIR images, hyperdense on CT scan and isointense on T1WI, showing exuberant postcontrast enhancement with few non enhancing hypointense areas. No blooming on SWI images. Facilitated diffusion. ICA is stretched and narrowed	Left cavernous hemangioma	Cavernous angioma
31	30/F	Left eye deviation, left eye vision loss	Left eyelid drooping for 3 months, left third, fourth, and sixth nerve palsy, left cavernous sinus lesion with hemangioma	It is hypodense on CT with punctate calcification	Left parasellar lesion having extension into the suprasellar region, left Meckel's cave and along the fifth nerve into the left preoptine cistern heterogeneously hyperintense on T2WI and partially inverting on FLAIR images, hypointense on T1WI and showing mild heterogeneous postcontrast enhancement. Blooming foci are seen on SWI images	Left trigeminal schwannoma. Possibly cystic DD: meningioma	Chordoma
32	56/F	Right eye ptosis, diplopia	-	ND	Right parasellar lesion with posterior fossa extension. Moderately hyperintense on T2WI and FLAIR images with homogenous moderate post-contrast enhancement. Dural tail is seen	Meningioma	Meningothelial meningioma
33	22/F	Right eyelid drooping diplopia	-	ND	Right parasellar lesion. Homogenous moderately hyperintense lesion on both T2WI and FLAIR images. Homogenous enhancement. Lobulated lesion with dural tail	Meningioma	Chordoid meningioma

Table 1 (Continued)

No.	Age/sex	Clinical features	O/E	CT	MRI	R/D	HPE
34	52/F	NA	Left cavernous sinus hemangioma	ND	Left parasellar large lesion with suprasellar extension. Appearing heterogeneously hyperintense on T2WI and FLAIR images with central hypointensity and hypointense on T1WI with heterogenous postcontrast enhancement (central nonenhancing area)	Meningioma	Cavernoma
35	67/F	Left eye ptosis, left face reduced sensation, reduced EOM	-	ND	Left parasellar lesion with suprasellar extension appearing moderately hyperintense on T2WI and FLAIR images. Hypointense on T1WI and homogenous post-contrast enhancement. Dural tail noted	Meningioma	Meningioma
36	45/F	Headache, drooping of right eyelid		ND	Right parasellar lesion with suprasellar and posterior fossa extension. Hyperintense homogeneously on T2WI and FLAIR images. Lobulated. Hypointense on T1WI. Homogenous enhancement. Dural tail noted. SWI images are not available	Meningioma	Hemangioma
37	57/F	Headache and vomiting	Right ophthalmoplegia right third and fourth nerve palsy, V1/V2/V3 sensory involvement	ND	Right parasellar lesion with superior orbital fissure extension. Well defined hyperintense lesion on both T2WI and FLAIR images and hypointense on T1WI and shows punctate enhancement on early postcontrast images. Few areas of hyperintensity are seen on T1WI and few areas of hypointensity are also seen on T2WI. The same areas are appearing hypointense on SWI but no blooming is seen	Cavernous hemangioma	Cavernous hemangioma
38	44/F	Left facial weakness years, left progressive vision loss	Left eye ptosis	ND	Moderately hyperintense on T2WI and FLAIR images with post-contrast enhancement	Left sided meningioma with ICA encasement	Fibrous meningioma

Abbreviations: CT, computed tomography; DD, differential diagnosis; EOM, extra ocular movements; F, female; FLAIR, fluid-attenuated inversion recovery; HPE, histopathological examination; ICA, internal carotid artery; O/E, on examination; M, male; MCA, middle cerebral artery; MRI, magnetic resonance imaging; NA, not available; ND, not done; R/D, radiodiagnosis; SWI, susceptibility weighted imaging; WI, weighted imaging.

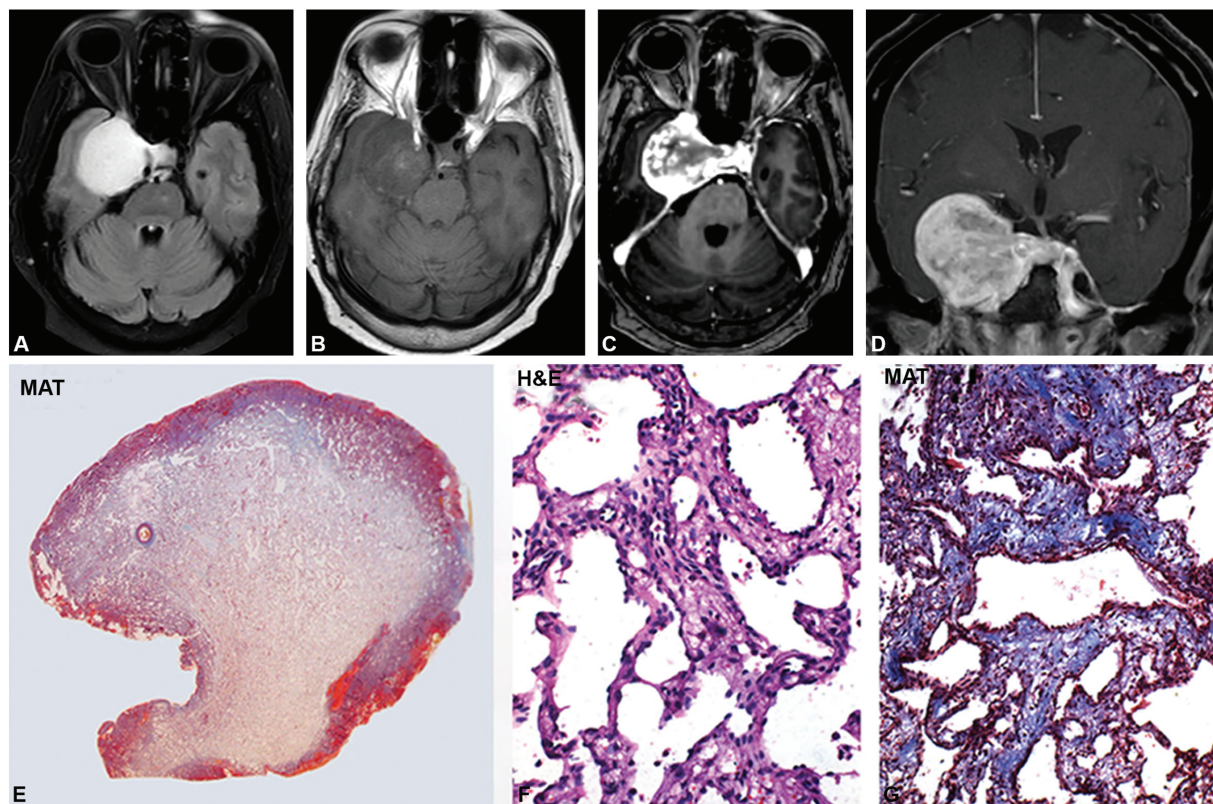


Fig. 1 Cavernous angioma. MR imaging shows left cavernous regional well-circumscribed lesion displaying brilliantly hyperintensity on T2WI and FLAIR image, iso to hypointense on T1WI (A, B) with exuberant enhancement on contrast administration (C, D) reminiscent of a meningioma. However central non-enhancing areas in the early phase (C) which enhanced in the delayed phase are characteristic of cavernous angioma. Histology revealed circumscribed, smooth-surfaced lesion (E) with characteristic back-to-back arranged thin venous channels with flattened endothelium (F) separated by thin fibrous stroma (G). (E, MAT $\times 8$; F, H&E $\times 10$; G, MAT $\times 10$). H&E, hematoxylin and eosin; MAT, Masson's trichrome; MR, magnetic resonance; WI, weighted imaging.

patulous and lacked thrombosis, calcification, and was devoid of hemosiderin. A single case that showed a sudden increase in the size of the lesion following pregnancy was positive for progesterone receptor in the lining endothelial cells but failed to express estrogen receptor.

Aspergilloma

Clinically, three cases presented with features of facial pain while one patient, in addition, had MCA infarct, ptosis, and visual loss (five cases, 13.51%; age range: 25–53 years, mean = 39.4 years). The mean duration of symptoms was 1 month. Total ophthalmoplegia was seen in one, and sensory loss in trigeminal nerve distribution area in two patients. Radiographically, the tumor appeared heterogeneously hyperdense on CT scan (**Fig. 2A**), heterogeneously hyperintense on T2WI, and FLAIR images with hypointense areas within, hypointense on T1WI, with heterogeneous postcontrast enhancement (**Fig. 2B–E**). Narrowing and stretching of the internal carotid artery (ICA) were noted. Bone destruction was evident in few lesions with no blooming seen on susceptibility weighted imaging (SWI) images. Histologically, the lesion revealed abundant necrotic debris, enclosed by broad fibrotic zones highlighted on Masson's trichrome stain (**Fig. 2F**) with dense lymphohistiocytic infiltrate and multinucleate giant cells (**Fig. 2G**) that contained ingested fragments of septate acute-angled branching hyphal forms

on periodic acid schiff and gomeri methenamine silver staining, morphologically resembling *Aspergillus spp.* (**Fig. 2H**).

Meningioma

Majority of the patients presented with ptosis and diplopia (80%) of 2 years' duration (five cases, 13.51%; age range: 44–67 years; mean = 49.2 years, all-female patients). Raised intracranial pressure, headache, visual disturbances, third nerve palsy, and left ophthalmic branch of trigeminal nerve causing hypoesthesia were noted in one case each. Radiographically, the tumor showed T1 hypointense (**Fig. 3A**) and T2 hyperintense, well-circumscribed, and solid with uniform contrast enhancement (**Fig. 3D**). Narrowing and stretching of the ICA was seen when the ICA was encased by the lesion (**Fig. 3E**). Few lesions also revealed a dural tail. Extension of the lesion along the nerve roots of the trigeminal nerve was evident. On neuroimaging, all four cases were concordant with histological diagnosis. Microscopically, various histological subtypes were noted (fibrous, meningothelial, chondroid, and angiomatous). The tumor showed meningothelial cells in lobules demarcated by predominant small to medium-sized thin-walled vascular channels (**Fig. 3F**). The tumor cells were largely uniform, with oval benign nuclei and delicate chromatin that showed occasional mitosis and expressed globally expressed epithelial membrane antigen (EMA) positivity (**Fig. 3F** inset).

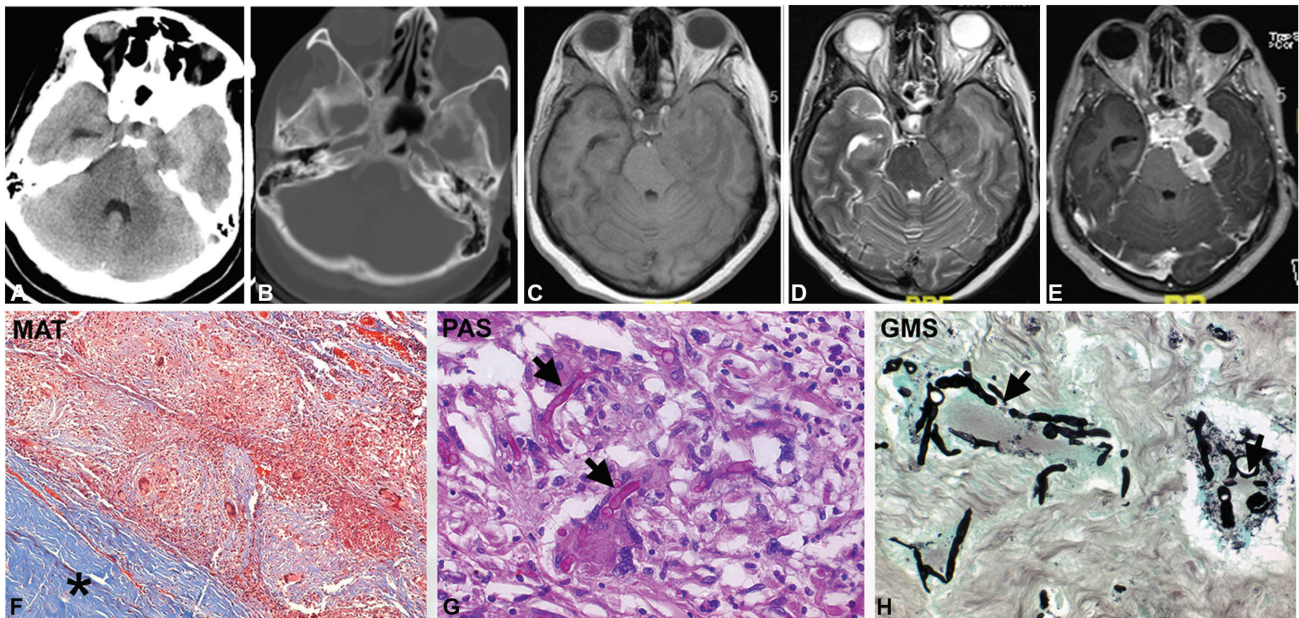


Fig. 2 Aspergilloma. CT scan plain (A), T1WI, T2WI and postcontrast images showing heterogeneous hyperdensity (A) at left cavernous sinus without bony destruction (A, B). It is hypointense on T2WI (C) with heterogenous postcontrast enhancement. Note the presence of edema in the left temporal parenchyma (D). The imaging diagnosis was meningioma. The lesion on histology revealed a granulomatous lesion extending along the dural wall (F) of the cavernous sinus. The giant cells had engulfed characteristic septate acute angled branching hyphae of *Aspergillus* spp. demonstrated by periodic acid-Schiff (PAS) (G) and Gomori's methenamine silver stains (GMS) (H). (F, MAT \times Obj. \times 4; G, PAS stain \times Obj. \times 20; H, GMS stain \times Obj. \times 20). CT, computed tomography; MAT, Masson's trichrome; WI, weighted imaging.

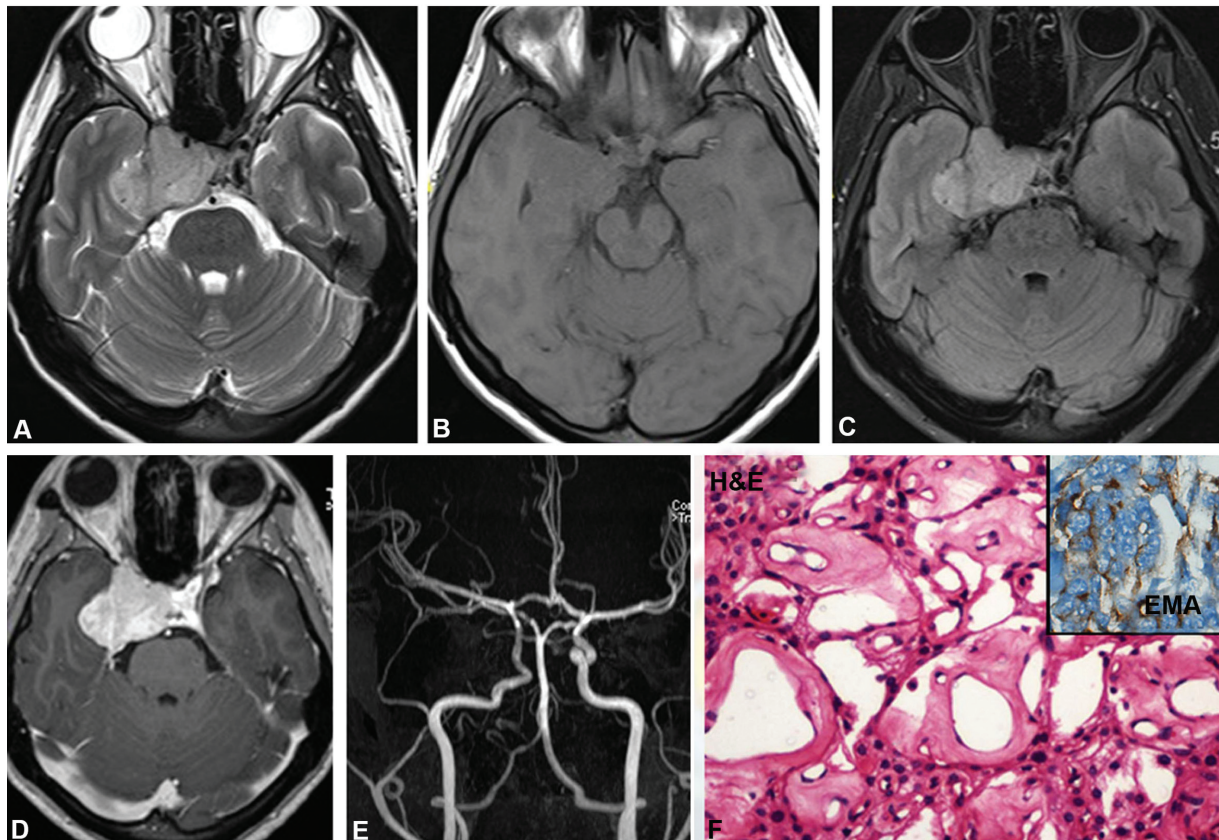


Fig. 3 Meningioma. T2WI, T1WI, FLAIR, postcontrast and MRA showing right cavernous sinus hyperintense lesion on T2WI and FLAIR (A–C), isointense on T1WI (B) with uniform post-contrast enhancement (D) characteristic of meningioma. Note right cavernous ICA is stretched and narrowed on MRA (A–D). Histology reveals an angiomatous meningioma with several thick hyalinized vessels (E). The tumor cells reveal membranous labeling for EMA (E, inset). (E, H&E \times Obj. \times 40; F, EMA \times Obj. \times 40). H&E, hematoxylin and eosin; FLAIR, fluid-attenuated inversion recovery; MRA, magnetic resonance angiogram; WI, weighted imaging.

Schwannoma

Patients presented with features of raised intracranial pressure with headache and diplopia (2 cases) of 2 years duration (three cases, 7.8%; age range: 19–28 years, mean = 22.3 years; M:F = 2:1). Clinical evaluation showed involvement of multiple cranial nerve (left third, fourth, and sixth nerves) causing palsy. Radiologically, the tumor showed heterogeneous signal intensity on T2WI and FLAIR images, with grossly hyperintense cystic areas and solid isointense areas on T2WI and FLAIR and heterogeneous postcontrast enhancement (►Fig. 4A–D). CT scan showed trigeminal nerve root involvement and enlargement of nerve root foramen. On neuroimaging, the diagnosis was accurate in two, whereas one was mistaken for meningioma. Microscopically, the tumor was highly vascular with spindle cells arranged in characteristic hyper- and hypocellular Antoni A and B areas (►Fig. 4E). Tumor cells expressed S-100 (►Fig. 4F) positivity on immunohistochemistry confirming its Schwannian origin.

Adenocarcinoma

Three cases of metastatic carcinoma were diagnosed (three cases, 7.89%; age range: 25–73 years, mean = 51 years, M:F = 2:1). Clinically the patients presented with features of raised intracranial pressure like headache, visual blurring,

cranial nerve palsies (second–fifth and 7th), and recurrent memory loss of 2 months' duration. Radiologically, the tumor was hypointense on T2WI and FLAIR images and isointense on T1WI showing uniform enhancement (►Fig. 5A–E). Extension and destruction of the adjacent structures including orbit, pituitary fossa, and petrous bone were evident. On neuroimaging, two of the three cases were mistaken for meningioma. Microscopically, the tumor was seen in lobules forming characteristic acini and solid nest of cells exhibiting moderate anaplasia with brisk mitosis and areas of necrosis (►Fig. 5F) and expressed cytokeratin positivity on immune staining (►Fig. 5F, inset).

Chondrosarcoma

Two cases were diagnosed (two cases, 5.26%; age range: 48–56 years, mean = 52 years). Clinically, the patients presented with diplopia, visual impairment, and one of the cases showed cranial nerve involvement (third–fifth). Neuroimaging revealed heterogeneously hyperintense on T2WI and FLAIR (not so hyperintense) with the appearance of septations within it, hypointense on T1WI with heterogenous enhancement with more nonenhancing areas (►Fig. 6A–F). Extension into foramen rotundum noted along the left maxillary nerve. No areas of blooming as noted. On

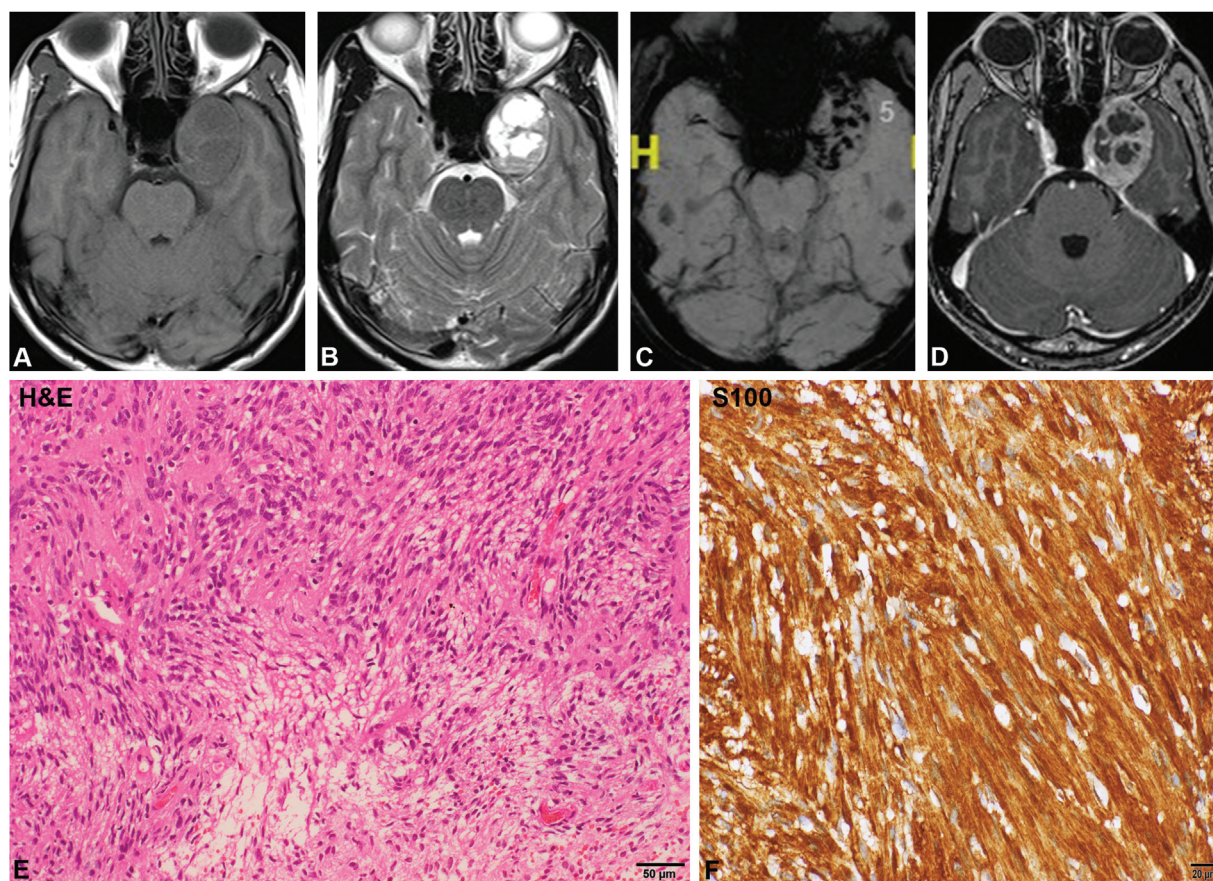


Fig. 4 Schwannoma. Left parasellar lesion hypointense on T1WI, T2WI, SWI, and postcontrast T1WI shows a heterogeneously hyperintense lesion on T2WI with cystic areas (A, B), and heterogenous post-contrast enhancement (D). SWI images are showing microbleeds (C) within the lesion characteristic of schwannoma (A–D). Histology reveals schwannoma with characteristic spindled cells with wavy nuclei arranged in compact and loose zones (E) with strong diffuse S-100 positivity confirming Schwannian origin (F). (E, H&E $\times 10$; F, S-100 $\times 20$). H&E, hematoxylin and eosin; SWI, susceptibility weighted imaging; WI, weighted imaging.

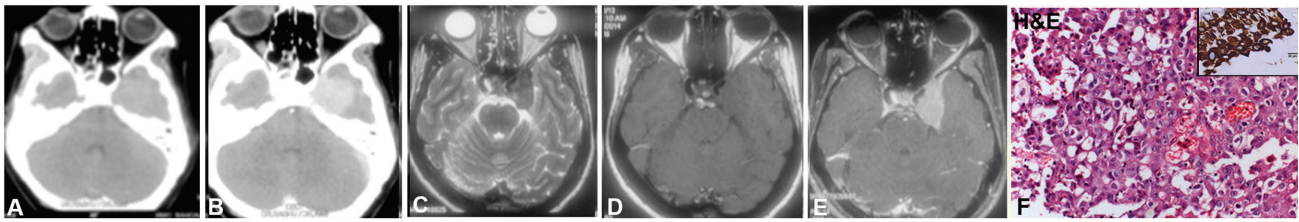


Fig. 5 Adenocarcinoma. CT plain and contrast study shows a mildly hyperdense enhancing lesion in right parasellar lesion (A, B). On MRI, the lesion is hypointense on T2WI, isointense on T1WI showing uniform contrast enhancement (C–E). Imaging possibility considered was meningioma. Histopathology revealed features of adenocarcinoma with neoplastic epithelial cells arranged in tubules and acini. (F, H&E \times Obj. \times 4). Immunostaining was strongly pan-cytokeratin positive (F) and negative for pituitary adenoma markers (images not shown). (F, H&E \times Obj. \times 20; F, inset: pan-cytokeratin \times Obj. \times 20). CT, computed tomography; H&E, hematoxylin and eosin; WI, weighted imaging.

neuroimaging, it was mistaken for schwannoma. Histologically the lesion showed lobulated chondroid lesion (\rightarrow Fig. 6G) with low-grade malignant chondrocytes (\rightarrow Fig. 6H), showing hyperchromasia, binucleation, and mitotic activity. The tumor was positive for S-100 (\rightarrow Fig. 6I) and negative for EMA and cytokeratin. Ki-67 / MIB-1 / mindbomb E3 ubiquitin protein ligase 1 labeling index was low.

Chordoma

A single case (2.63%) was recorded in a 30-year-old female presenting with dropping of the eyelid, vision impairment due to involvement of cranial nerves (third, fourth, and sixth). The tumors were hypodense on CT with punctate calcification, heterogeneously hyperintense on T2WI showing few cystic areas within, and partially inverting on FLAIR images. It was hypointense on T1WI with areas of hyperintensity within showing mild heterogeneous postcontrast enhancement (\rightarrow Fig. 7A–E). Foci of blooming were seen on SWI images. CT scan revealed destruction of the apex of the right petrous bone

with superior clivus. On neuroimaging, both the cases were diagnosed as schwannoma. Histologically, a lobulated lesion composed of cells with epithelioid morphology arranged in characteristic chords separated by bubbly mucoid stroma was seen with scattered physaliphorous cells with abundant multivacuolated cytoplasm (\rightarrow Fig. 7F). Immunohistochemistry revealed positivity for S-100 (\rightarrow Fig. 7G), EMA, and cytokeratin (\rightarrow Fig. 7H) confirming the diagnosis.

Discussion

Cavernous sinus is a small space located at parasellar region having a carotid artery, venous plexus, nerves, and sympathetic nerves. The spectrum of lesions includes infectious (bacterial and fungal), inflammatory, vascular, and neoplastic entities that can cause cavernous sinus syndrome.⁴ Primary tumors of the cavernous sinus may be located in intracavernous or interdural space. The lateral wall of the cavernous sinus is composed of an inner membranous layer

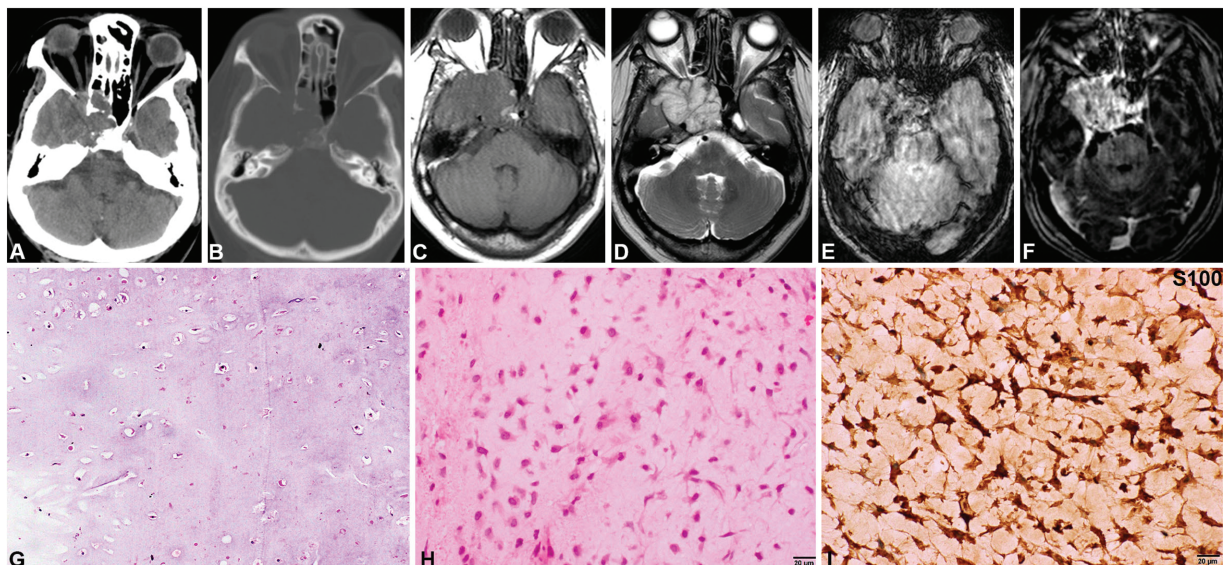


Fig. 6 Chondrosarcoma. CT scan and bone windows show hypodense lesion with calcification and destruction of the left side of the clivus and sellar floor (A, B). The lesion is hypointense on T1WI (C), Hyperintense on T2WI with calcification with Postcontrast Enhancement. T2WI, VenoBOLD and postcontrast images of right cavernous sinus lesion (A–F). The possibility of schwannoma was considered on imaging. Histology revealed a chondroid neoplasm with chondrocytes within lacunae (G), displaying increased cellularity and mild atypia but low mitotic activity characteristic of low-grade chondrosarcoma (H). Tumor cells exhibiting strong S-100 positivity confirming chondroid origin (I). (G, H&E \times Obj. \times 10; H, H&E \times Obj. \times 20; I, S100 \times Obj. \times 20). CT, computed tomography; H&E, hematoxylin and eosin; WI, weighted imaging.

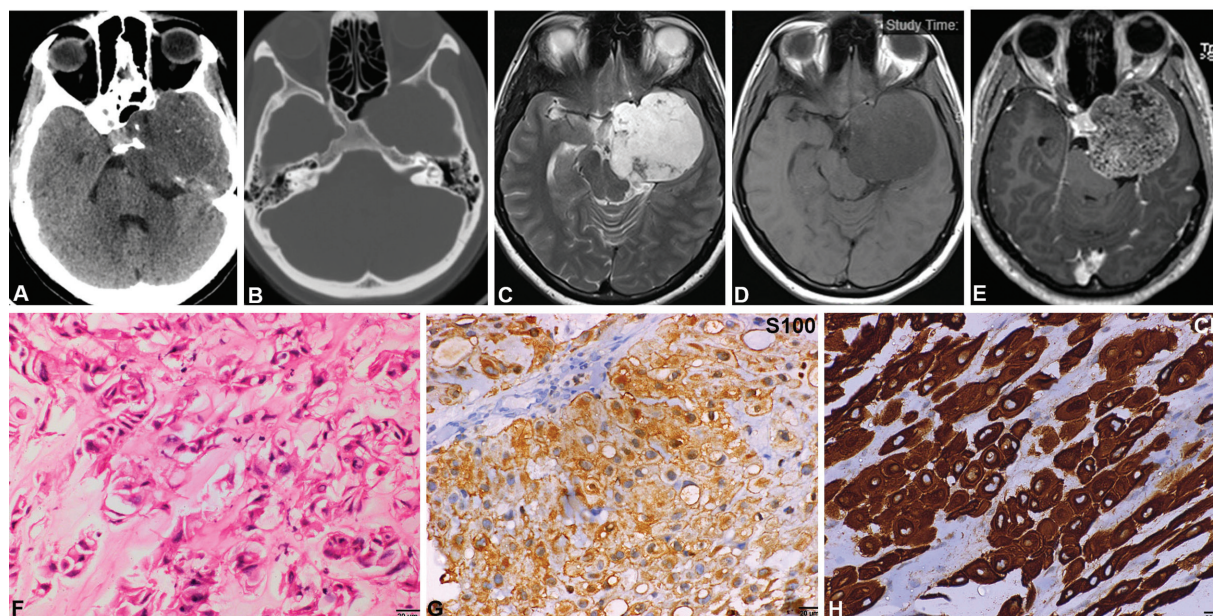


Fig. 7 Chordoma. Left parasellar lesion on CT scan appears hypodense. Note the absence of any bony destruction (A, B). On MRI it is hyperintense on T2WI (C), hypointense on T1WI (D) with heterogenous post-contrast enhancement (E). Based on these features, the possibility of schwannoma was suspected. Histology revealed a lobulated tumor showing distinctive cells with epithelioid morphology arranged in chords separated by bubbly mucoid stroma and characteristic physaliphorous cells with abundant multivacuolated cytoplasm. (F), tumor cell express S-100 (G) and strong cytokeratin confirming the diagnosis of chordoma (H). (F, H&E \times Obj.40x; G, S100 \times Obj.20; H, pan-cytokeratin \times Obj.20). CT, computed tomography; H&E, hematoxylin and eosin; MRI, magnetic resonance imaging; WI, weighted imaging.

and an outer dura propria, continuous with the tentorium. The interdural space is a potential space from which various tumors including neurinomas of the cranial nerves (fifth and less likely third, fourth, and sixth), epidermoid tumors, melanomas, cavernous angiomas, meningiomas, and hemangiopericytomas arise.¹⁰ All these lesions tend to displace cranial nerves laterally compress causing palsy and ensheath the carotid artery potentially manifest as cavernous sinus syndrome. Several individual case studies describing pathology and radiological features of cavernous sinus lesions are reported in the literature.^{1,6,8,11,12} The largest series published by Jefferson documented 112 cavernous sinus lesions, composed of 52 tumors, 38 aneurysms, and 22 cases of carotid-cavernous fistulae. The majority of the tumors in the Jefferson series were secondary extensions from the nasopharynx or paranasal sinus lesions.¹³ To the best of our knowledge, this is the first study enumerating the pathological and imaging spectrum of surgically resected cavernous sinus lesions.

Cavernous Angioma

Cavernous angiomas are uncommon in extra-axial locations and the majority of them are located in the intra-axial portion of the middle cranial fossa. Reported cases at extra-axial locations include the optic chiasm, perimesencephalic cistern, internal auditory canal, cerebellar pontine angles. Extra-axial intracranial cavernous hemangiomas at cavernous sinus were representing 0.4 to 2% of all dural-based haemangiomas.¹⁴ Shi et al reported female preponderance and mean age of presentation in the fifth decade.¹⁵ In our series, it was the most frequent lesion of cavernous sinus (50%) and female predominance was noted, the tumors

occurred at a younger age, in the third decade. Secondary involvement of the oculomotor cranial nerve at the lateral wall of the cavernous sinus wall is a frequent manifestation observed in the present study. In MRI, they appear well-circumscribed, exuberantly hyperintense on T2WI and FLAIR and hypointense on T1WI with heterogenous brilliant contrast enhancement in early postcontrast images. Nonenhancing regions in the early phase show enhancement in the delayed images, a feature seen in some of our cases. They tend to scallop the bone without destroying them. At times, they could not be reliably distinguished preoperatively from meningiomas because of homogenous hyperintensity on T2WI which is a characteristic of the angiomatous and microcystic variants of meningiomas. In such scenarios, other features such as a dural tail, narrowing and stretching of the involved cavernous ICA, and angiography (DSA [digital subtraction angiography]) images showing early enhancement are pointers that favor meningioma.^{16–18} In our series, discordance rate was 22.22% (4/18 cases). The majority of them were mistaken for meningioma (three cases) due to dural tail and narrowing of the ICA. The presence of vascular enhancement along the tentorium may be mistaken for the dural tail on MRI. Sometimes when the hemangioma is very large, it can compress and narrow down the ICA and surgical excision becomes difficult due to excessive bleeding; tendency to invade middle cranial fossa, sellar regions, and encase neurovascular structures^{11,19–21} are the other hindering factors for complete excision. Intra- and postoperative excessive bleeding leading to mortality has been documented up to 12.5%.²² Unlike hemangioma, trigeminal schwannoma of the middle fossa tends to be centered slightly more posteriorly¹⁶ and displaces carotid artery,

cranial nerves inside the cavernous sinus or the petrous bone, rather than ensheathing them; thereby preservation of these structures during surgery is possible. Several surgical approaches can be used to excise the tumor completely for excellent results at the sellar/parasellar area.²³ On imaging, there showed heterogeneous signal characteristics on both T1WI and T2WI, appearing hyperintense on T2WI and hypointense on T1WI. They showed cystic areas within with heterogeneous postcontrast enhancement. No delayed enhancement is seen. Microbleeds are evident within the lesion on gradient or SWI images. They have a propensity to spread along trigeminal nerve branches; however, this feature is not a specific feature of nerve sheath tumors. It may be seen in meningioma, fungal granulomas, and metastasis. Prominent cystic degeneration, foamy macrophages, hemorrhage, hemosiderin-laden macrophages, dystrophic calcification, and perivascular hyalinization of vessels are clues for the diagnosis of schwannoma. In our series, there were only three cases of schwannomas arising from the cavernous sinus, and all were accurately diagnosed on imaging and did not pose any difficulty. Meningiomas can arise from the cavernous sinus lateral wall dura or the dura or from dural coverings of sphenoid/petrous bone. Ambiguous imaging findings and mass effect producing lesions necessitate surgical intervention and histological confirmation for definitive management. They appear homogeneously hyperintense on T2WI and FLAIR and iso- to hypointense on T1WI showing uniform enhancement. Other features include dural tail, bony remodeling, compression, and narrowing of the cavernous sinus. ICA and angiography detection of “sunburst” pattern with early staining and delayed washout help in differentiating meningiomas from other lesions. Benign nonmeningothelial tumors have got better surgical clearance compared with meningiomas, hence they cause a lower rate of preoperative nerve deficits and postoperative ocular deficits.¹⁶ Surgical and radiosurgical interventions are found to be complementary to each other. The deciding factors for the selection of treatment modality are the size and volume of haemangiomas.²⁴

Aspergillosis was the second most frequent lesion on our series of CS lesions (13.5%): cavernous sinus involvement occurs by direct extension or hematogenous spread. The common primary site involvement includes paranasal sinuses, ear cavity, and orbit. Pathogenesis includes necrotizing vasculitis causing thrombosis and infarction in immunocompromised patients favoring the rapid spread of the inflammation to the cranial cavity.²¹ They show nonenhancing areas with exuberant enhancement. The presence of perilesional edema in the temporal lobe structures, bony destruction, extension, and involvement of the structures of the infratemporal fossa (across various parapharyngeal spaces) assist in imaging diagnosis of fungal infection. Involvement and extension from the paranasal sinuses is an important clue for diagnosis. Paramagnetic elements like iron and magnesium derived from hemorrhage or aspergillus fungal colonies brings about characteristic reduced signal intensity on T1WI and very low signal intensity on T2WI are characteristic findings in paranasal sinus aspergillosis.^{25,26}

Adenocarcinoma

Metastases to the cavernous sinus are uncommon and the incidence of central nervous system (CNS) involvement is approximately 30 to 40% of systemic cancer patients.²⁷ Thomas and Yoss recorded 23% parasellar lesion to be metastatic tumors.^{27,28} The role of biopsy and surgical resection in known systemic cancer and MRI-confirmed cavernous sinus lesions is unclear.²⁹ Various reported primary tumors in literature includes squamous cell carcinoma (SCC) of the head and neck,³⁰ nasopharyngeal carcinoma,³¹ oropharyngeal carcinoma,³¹ melanoma,³² papillary adenocarcinoma,³³ rhabdomyosarcoma of the head and neck,^{34,35} salivary gland duct carcinoma, and SCC of salivary glands.^{30,34,35} MRI plays an important role in diagnosing and describes the extent of the lesion. They appear hypointense on both T2WI and FLAIR with bony destruction and extension showing uniform postcontrast enhancement. Perineural extension with involvement of various parapharyngeal spaces and loss of normal fat planes are evident. Histopathological evaluation is essential for confirmation of diagnosis.³⁶ In our series, two of three cases were not suspected on imaging due to lack of known primary malignancy, involvement limited to cavernous sinus area and absence of bony destruction.

Cranial chondrosarcomas are slow-growing invasive lesions arising from the skull base, most common at the petrooccipital synchondrosis, and can extend to involve the cavernous sinus. On imaging, these lesions showed high signal intensity on T2W MR images because of the chondroid matrix.³⁷ Regions of low signal intensity can be depicted owing to calcifications. The lesions usually show marked enhancement on gadolinium-enhanced MR images. CT demonstrates matrix calcification in a chondroid pattern (“ring and arc” pattern) and helps in the assessment of bone destruction. In our series, both the cases were misdiagnosed as schwannoma, as there was no bony destruction and revealed septations with marked gadolinium enhancement.³⁸

Chordomas are malignant midline lesions arising from notochord rest cells of the axial skeleton showing local aggressiveness and clival bone involvement in the cranium. They are seen in the fourth decade and may be off-centered in the cavernous sinus region mimicking other mass lesions. In our series, there was one case and misdiagnosed as schwannoma due to its off-center location, absence of bony destruction, and presence of blooming foci on SWI images. On MRI, they mimic the chondrosarcoma appearing heterogeneously hyperintense with cystic areas on T2WI and hypointense on T1WI showing heterogenous mild postcontrast enhancement. They are hypodense on CT scans and show stippled calcifications and bony destruction.³⁹ Differential diagnosis includes chondrosarcoma chordoid meningioma and other look-alike myxoid lesions (extraskelatal myxoid chondrosarcoma, myxoid liposarcoma, and myxopapillary ependymoma). Epithelial markers’ positivity (cytokeratin) is a feature of chordoma and absent in other myxoid sarcomas and ependymomas. On histology, presence of physaliphorous cells is a clue for chordoma diagnosis.⁴⁰ Low-grade chondrosarcoma needs immunohistochemistry

assistance, as it lacks pleomorphism, hyperchromasia, and infiltrative features, the other clues include binucleation and clusters of malignant-looking chondrocytes within a single lacuna extensive sampling of the entire specimen is essential for confirmation of grade.³⁹

Conclusion

The pathological spectrum of mass lesions in the cavernous sinus is highly diverse. This is the first study to enumerate the pathological and neuroimaging spectrum of surgically resected cavernous sinus lesions. The majority of lesions were cavernous hemangiomas (50%), followed by aspergilloma, meningioma, and schwannoma. Metastases and bony lesions such as chordoma and chondrosarcoma were rare. Neuroimaging findings are essential for initial diagnosis and to describe the extent of the lesion. However, histopathological evaluation is essential in the diagnosis of lesions of cavernous sinus as imaging may not always be definitive. In our study, cavernous hemangiomas, metastases, and chordomas, and chondrosarcoma posed the greatest difficulty in diagnosis. In the context of clinical and neuroimaging discordance in diagnosis, pathological characterization becomes essential for appropriate and timely management.

Ethical Approval

This is a retrospective type of study and hence, formal consent is not required. The present article is a study on surgically resected human tissues and does not involve experiments on human participants performed by any of the authors.

Funding

None.

Conflict of interest

None declared.

Acknowledgment

The authors would like to thank the doctors who referred their cases to our department for neuropathological diagnosis. The authors also acknowledge the technical assistance of all technical staff of the Department of Neuropathology, National Institute of Mental Health & Neurosciences (NIMHANS), Bangalore, Karnataka, India, and Mr. Manjunath kemparama, for assistance with photographic montages.

References

- Larson TL. Petrous apex and cavernous sinus: anatomy and pathology. *Semin Ultrasound CT MR* 1993;14(03):232–246
- Keane JR. Cavernous sinus syndrome. Analysis of 151 cases. *Arch Neurol* 1996;53(10):967–971
- Razek AA, Castillo M. Imaging lesions of the cavernous sinus. *AJNR Am J Neuroradiol* 2009;30(03):444–452
- Nakamura M, Krauss JK. Image-guided resection of small lesions in the cavernous sinus and Meckel's cave. *Eur J Surg Oncol* 2010;36(02):208–213
- Fratzoglou M, Condilis N, Panayiotopoulos V, Bahal D, Patheni M. Cavernous sinus chondroma. Case report and review of the literature. *Ann Ital Chir* 2008;79(01):43–45
- Gharabaghi A, Koerbel A, Samii A, Safavi-Abbasi S, Tatagiba M, Samii M. Epidermoid cysts of the cavernous sinus. *Surg Neurol* 2005;64(05):428–433, discussion 433
- Ladziński P, Majchrzak H, Maliszewski M, et al. Direct and remote outcome after treatment of tumours involving the cavernous sinus and its surroundings. *Neurol Neurochir Pol* 2008;42(05):402–415
- Sohn CH, Kim SP, Kim IM, Lee JH, Lee HK. Characteristic MR imaging findings of cavernous hemangiomas in the cavernous sinus. *AJNR Am J Neuroradiol* 2003;24(06):1148–1151
- Vogl TJ, Schick C, Mack M, Gstöttner W. Diagnostic imaging and differential diagnosis of pathological processes of the sinus cavernosus [in German]. *Radiologe* 2003;43(02):161–170
- el-Kalliny M, van Loveren H, Keller JT, Tew JM Jr. Tumors of the lateral wall of the cavernous sinus. *J Neurosurg* 1992;77(04):508–514
- Heth JA, Al-Mefty O. Cavernous sinus meningiomas. *Neurosurg Focus* 2003;14(06):e3
- Lee AG, Miller NR, Brazis PW, Benson ML. Cavernous sinus hemangioma. Clinical and neuroimaging features. *J Neuroophthalmol* 1995;15(04):225–229
- Jefferson G. The Bowman Lecture. Concerning injuries, aneurysms, and tumors involving the cavernous sinus. *Trans Ophthalmol Soc U K* 1953;73:117–152
- Ohata K, El-Naggar A, Takami T, et al. Efficacy of induced hypotension in the surgical treatment of large cavernous sinus cavernomas. *J Neurosurg* 1999;90(04):702–708
- Shi J, Hang C, Pan Y, Liu C, Zhang Z. Cavernous hemangiomas in the cavernous sinus. *Neurosurgery* 1999;45(06):1308–1313, discussion 1313–1314
- Eisenberg MB, Al-Mefty O, DeMonte F, Burson GT. Benign non-meningeal tumors of the cavernous sinus. *Neurosurgery* 1999;44(05):949–954, discussion 954–955
- Meyer FB, Lombardi D, Scheithauer B, Nichols DA. Extra-axial cavernous hemangiomas involving the dural sinuses. *J Neurosurg* 1990;73(02):187–192
- Momoshima S, Shiga H, Yuasa Y, Higuchi N, Kawase T, Toya S. MR findings in extracerebral cavernous angiomas of the middle cranial fossa: report of two cases and review of the literature. *AJNR Am J Neuroradiol* 1991;12(04):756–760
- Rigamonti D, Pappas CTE, Spetzler RF, Johnson PC. Extracerebral cavernous angiomas of the middle fossa. *Neurosurgery* 1990;27(02):306–310
- Sawamura Y, de Tribolet N. Cavernous hemangioma in the cavernous sinus: case report. *Neurosurgery* 1990;26(01):126–128
- Suzuki Y, Shibuya M, Baskaya MK, et al. Extracerebral cavernous angiomas of the cavernous sinus in the middle fossa. *Surg Neurol* 1996;45(02):123–132
- Aversa do Souto A, Marcondes J, Reis da Silva M, Chimelli L. Sclerosing cavernous hemangioma in the cavernous sinus: case report. *Skull Base* 2003;13(02):93–99
- Srinivas D, Somanna S, Ashwathnarayana CB, Bhagavatula ID. Multicompartmental trigeminal schwannomas: management strategies and outcome. *Skull Base* 2011;21(06):351–358
- Srinivas D, Sarma P, Shukla D, et al. Multimodality management of cavernous sinus hemangiomas—an institutional experience. *J Neurol Surg B Skull Base* 2017;78(05):399–407
- Yamada K, Zoarski GH, Rothman MI, Zagardo MT, Nishimura T, Sun CC. An intracranial aspergilloma with low signal on T2-weighted images corresponding to iron accumulation. *Neuroradiology* 2001;43(07):559–561
- Chan LL, Singh S, Jones D, Diaz EM Jr., Ginsberg LE. Imaging of mucormycosis skull base osteomyelitis. *AJNR Am J Neuroradiol* 2000;21(05):828–831

- 27 Kumar R, Deopujari CE, Shah R, Kumar A. Metastatic adenocarcinoma of bilateral cavernous sinus and optic nerve with unknown primary mimicking orbital pseudotumor. *Neurol India* 2009; 57(01):82–84
- 28 Thomas JE, Yoss RE. The parasellar syndrome: problems in determining etiology. *Mayo Clin Proc* 1970;45(09):617–623
- 29 Panigrahi M, Arun P, et al. Uncommon cavernous sinus lesions: a review. *Progr Clin Neurosci* 2007;22:237–247
- 30 Urban SD, Hall JM, Bentkover SH, Kadish SP. Salivary duct carcinoma of minor salivary gland origin: report of a case involving the cavernous sinus. *J Oral Maxillofac Surg* 2002;60(08):958–962
- 31 de Bree R, Mehta DM, Snow GB, Quak JJ. Intracranial metastases in patients with squamous cell carcinoma of the head and neck. *Otolaryngol Head Neck Surg* 2001;124(02):217–221
- 32 Chang PC, Fischbein NJ, McCalmont TH, et al. Perineural spread of malignant melanoma of the head and neck: clinical and imaging features. *AJNR Am J Neuroradiol* 2004;25(01):5–11
- 33 Takami T, Ohata K, Tsuyuguchi N, et al. Cavernous sinus metastasis from thyroid papillary adenocarcinoma. *J Clin Neurosci* 2002; 9(05):598–600
- 34 Bumpous JM, Maves MD, Gómez SM, Levy BK, Johnson F. Cavernous sinus involvement in head and neck cancer. *Head Neck* 1993; 15(01):62–66
- 35 Reynard M, Brinkley JR Jr. Cavernous sinus syndrome caused by rhabdomyosarcoma. *Ann Ophthalmol* 1983;15(01):94–97
- 36 Nadarajah J, Madhusudhan KS, Yadav AK, Chandrashekhara SH, Kumar A, Gupta AK. MR imaging of cavernous sinus lesions: pictorial review. *J Neuroradiol* 2015;42(06):305–319
- 37 Korten AG, ter Berg HJ, Spincemaille GH, van der Laan RT, Van de Wel AM. Intracranial chondrosarcoma: review of the literature and report of 15 cases. *J Neurol Neurosurg Psychiatry* 1998;65 (01):88–92
- 38 Mahalingam HV, Mani SE, Patel B, et al. Imaging spectrum of cavernous sinus lesions with histopathologic correlation. *Radio-graphics* 2019;39(03):795–819
- 39 Radner H, Katenkamp D, Reifenberger G, Deckert M, Pietsch T, Wiestler OD. New developments in the pathology of skull base tumors. *Virchows Arch* 2001;438(04):321–335
- 40 Ferlito A, Recher G. Chondrometaplasia of the larynx. *ORL J Otorhinolaryngol Relat Spec* 1985;47(04):174–177